Novel channel models for visible light communications

Farshad Miramirkhani, Murat Uysal, Erdal Panayirci

Farshad Miramirkhani, Murat Uysal, Erdal Panayirci, "Novel channel models for visible light communications," Proc. SPIE 9387, Broadband Access Communication Technologies IX, 93870Q (7 February 2015); doi: 10.1117/12.2077565

SPIE.

Event: SPIE OPTO, 2015, San Francisco, California, United States

Novel Channel Models For Visible Light Communications[1]

Farshad Miramirkhani*[a], Murat Uysal[a], Erdal Panayirci[b]
[a]Department of Electrical and Electronics Engineering, Ozyegin University, Istanbul, Turkey;
[b]Department of Electrical and Electronics Engineering, Kadir Has University, Istanbul, Turkey

ABSTRACT

In this paper, we investigate channel modeling for visible light communications (VLC) using non-sequential ray tracing simulation tools. We create three dimensional realistic simulation environments to depict indoor scenarios specifying the geometry of the environment, the objects inside, the reflection characteristics of the surface materials as well as the characteristics of the transmitter and receivers, i.e., LED sources and photodioes. Through ray tracing simulations, we compute the received optical power and the delay of direct/indirect rays which are then used to obtain the channel impulse response (CIR). Following this methodology, we present CIRs for a number of indoor environments including empty/furnished rectangular rooms with different sizes and wall/object materials (e.g., plaster, gloss paint, wood, aluminum metal, glass) assuming deployment of both single and multiple LED transmitters. We further quantify multipath channel parameters such as delay spread and channel DC gain for each configuration and provide insights into the effects of indoor environment parameters (e.g., size, wall/object materials, etc.), transmitter/receiver specifications (e.g., single vs. multiple transmitters, location, rotation etc.) on the channel.

Keywords: Visible light communications, ray tracing, channel modeling, spectral reflectance

1. INTRODUCTION

There is an ever-increasing demand for wireless applications and services. Due to spectrum scarcity, conventional radio frequency (RF) solutions are not able to cope with this increasing demand. Low cost and highly reliable alternative and/or complementary solutions are required to enable a seamless wireless experience. Visible light communications (VLC) [1] has such a promise and depends on the dual use of the existing illumination infrastructure (i.e., LEDs) for wireless communication purposes. The human eye perceives only the average intensity when light changes fast enough, therefore LEDs can transmit data without a noticeable effect on the lighting output and the human eyes.

There is a growing literature on VLC spanning from advanced physical layer techniques to networking, see e.g., [2-6] and the references therein. Despite this increasing attention on VLC systems, there is a lack of proper visible light (VL) channel models. This is a serious concern since channel modeling is the very first step for efficient, reliable and robust VLC system design. In the current literature, the channel models developed for infrared (IR) in the past [7-9] are widely used in the analysis and design of VLC systems without a solid justification [10-12]. It should be noted that there are some significant differences between IR and VL communications. For example, an IR source can be approximated as a monochromatic emitter while a white light LED source is inherently wideband (380-780nm). This calls for the inclusion of wavelength-dependency of source in VLC channel modeling. Furthermore, in IR communication, the reflectance of materials is typically modeled as a constant. On the other hand, the reflectance of materials in the VL spectrum should be taken into consideration due to the wideband nature of VLC link.

In an effort to address this research gap in the literature, our recent work in [13] has used ray tracing approach to present realistic VLC channel models and associated characteristics for a number of indoor environments. Our study is based on Zemax®; a commercially available optical and illumination design software [14]. Although the main purpose of such software is optical and illumination system design, we take advantage of the ray tracing features of this software which allows an accurate description of the interaction of rays emitted from the lighting source within a specified confined

[1] This work is supported by TUBITAK Research Grant No. 113E307.

Broadband Access Communication Technologies IX, edited by Benjamin B. Dingel, Katsutoshi Tsukamoto,
Proc. of SPIE Vol. 9387, 93870Q · © 2015 SPIE · CCC code: 0277-786X/15/$18 · doi: 10.1117/12.2077565

space (i.e., room, office, etc). Our work in [13] is however limited to a small number of scenarios and single transmitter deployment. In this paper, we extend our earlier work in several directions. We consider various wall and furniture materials (i.e., plaster, gloss paint, wood, aluminum metal, glass), transmitter specifications (i.e., single vs. multiple transmitters, array type), and receiver specifications (i.e., location, rotation). Furthermore, we present IR channel models for the same environments as benchmarks to emphasize the differences between VL and IR models.

The remainder of the paper is organized as follows. In Section 2, we describe the methodology adopted for channel modeling. In Section 3, we present our CIR results for a number of indoor environments and quantify some main channel parameters. We finally conclude in Section 4.

2. METHODOLOGY

In our study, we use Zemax® which is an optical and illumination design software with sequential and non-sequential ray-tracing capabilities [14]. It allows an accurate description of the interaction of rays emitted from the LEDs for a user-defined environment. The simulation environment is created in Zemax® and enables us to specify the geometry of the environment, the objects inside, the reflection characteristics of the surface materials as well as the specifications of the sources (i.e., LEDs) and receivers (i.e., photodiodes).

2.1 Indoor Environments

In our work, we consider 15 different configurations illustrated in Fig. 1. The main features of these configurations are summarized below:

(1) Empty rectangular room with single transmitter located at the center of the ceiling and single receiver located at the center of the floor.

(2) Empty rectangular room with four transmitters located at the ceiling and single receiver located at the center of the floor.

(3) Empty rectangular room with single transmitter located at the center of the ceiling and single receiver located at the midway on the diagonal which stretches from the corner to the middle of the floor.

(4) Empty rectangular room with single transmitter located at the center of the ceiling and single receiver located at the corner of the floor.

(5) Empty rectangular room with single transmitter located at the center of the ceiling and single receiver (with rotation) located at the midway on the diagonal which stretches from the corner to the middle of the floor.

(6) Empty rectangular room with single transmitter located at the center of the ceiling and single receiver (with rotation) located at the corner of the floor.

(7) Rectangular room with a desk located at the corner of the room, four transmitters located at the ceiling and single receiver located on the desk.

(8) Rectangular room with a desk located at the corner of the room, four transmitters located at the ceiling, desk light (as an additional transmitter) located on the desk, and single receiver located on the desk.

(9) Empty rectangular room with single transmitter located at the center of the ceiling and single receiver located at the center of the floor. This is identical to configuration (1) except the fact that the floor material is different.

(10) Empty rectangular room with two transmitters located at the ceiling and single receiver located at the center of the floor.

(11) Empty rectangular room with four transmitters located at the ceiling and single receiver located at the center of the floor. This configuration differs from (2) since the coordinates of four transmitters are different from those in (2).

(12) Empty rectangular room with eight transmitters located at the ceiling and single receiver located at the center of the floor.

(13) Empty rectangular room with sixteen transmitters located at the ceiling and single receiver located at the center of the floor.

(14) Empty rectangular room with four transmitters located at the ceiling and single receiver located at the corner of the room. This configuration differs from (2) since the size of the room is different.

(15) Furnished rectangular room with four transmitters located at the ceiling and single receiver located at the corner of the room. The size of this room is the same as in (14). In this configuration, CAD objects available at [15] are used to model the furniture.

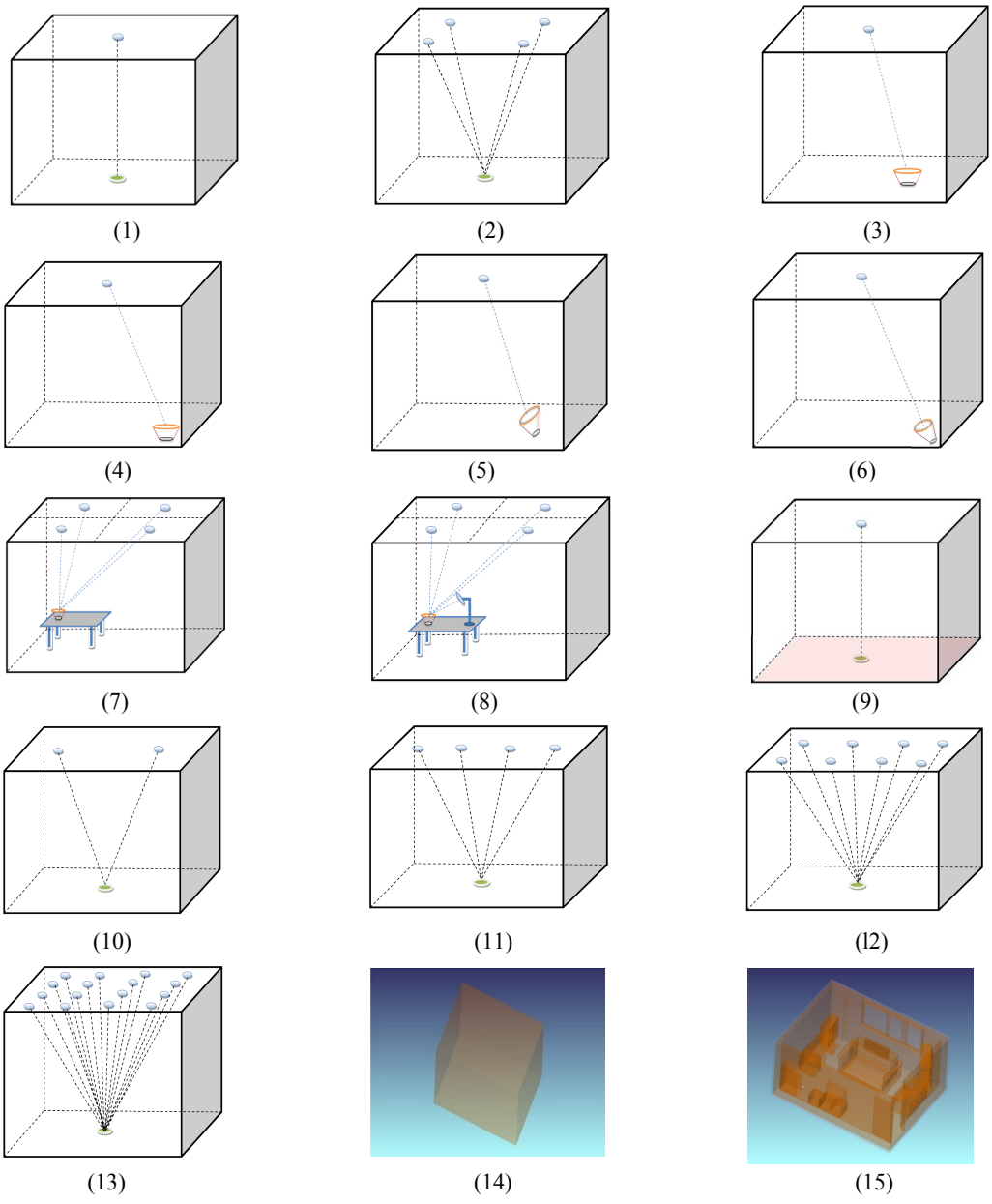

Figure 1. Different configurations under consideration

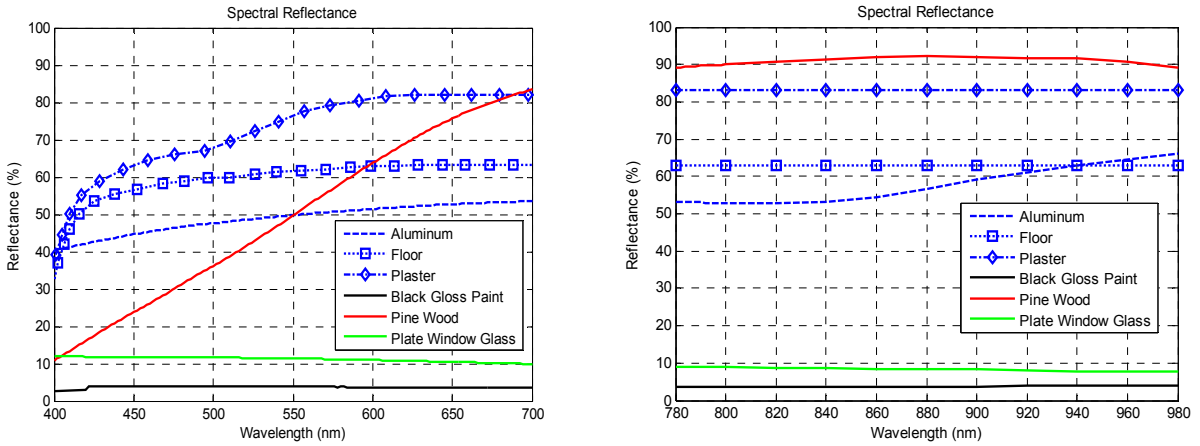

Figure 2. Spectral reflectance of materials used for walls, ceiling, floor and furniture (a) in VL band (b) in IR band

The exact positions of transmitters and receivers along with room sizes are provided in the Appendix. In our study, we assume that the walls and ceiling are plaster while the floor is pine wood. Furthermore, we assume that the desk, desk lamp, window, TV and radiators are respectively pine wood, black gloss paint, glass, black gloss paint and aluminum metal. These values are adopted from [16], [17] and are shown in Figure 2. As observed from Figure 2, the reflectance of most materials in IR band are nearly constant while the reflectance is highly dependent on wavelength in the VL band. To take this into account, we use "table coating method" in Zemax® and define a coating for each material that includes reflectivity versus wavelength values to realistically reflect this wavelength dependency.

2.2 Source

In our simulations, we use a Cree Xlamp® MC-E White LED with Lambertian distribution and a viewing angle of 110° [18] for VLC system. For comparison purposes, we also consider an IR source, specifically OSRAM® SFH 4283 IR 880 nm LED with same viewing angle and Lambertian distribution [19]. These source models are available at Radiant Zemax® online source library [14]. Figure 3.a. and 3.b. depicts relative power distribution of VL and IR LEDs respectively within their working wavelength range.

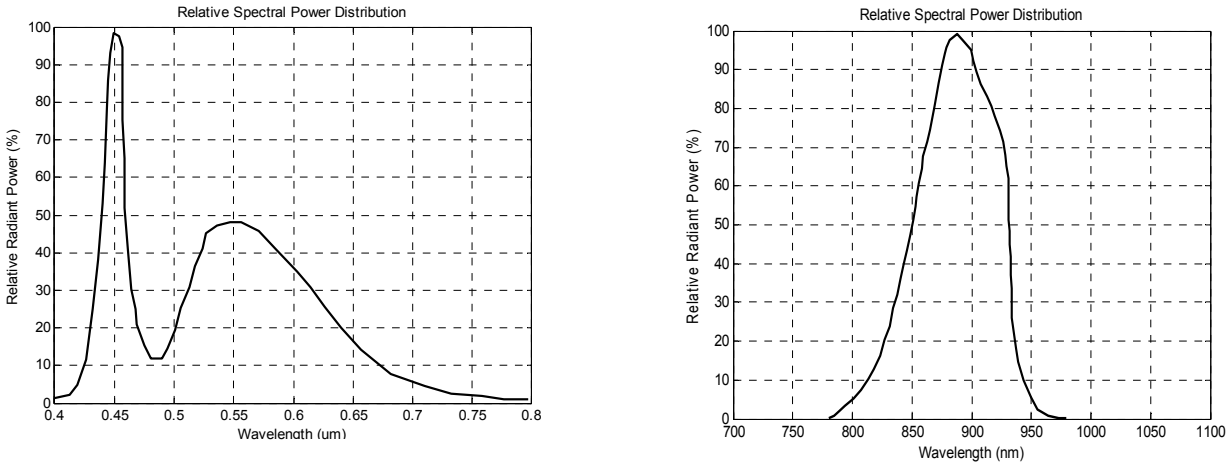

Figure 3. (a) relative spectral power distribution of Cree Xlamp® MC-E White LED (b) relative spectral power distribution of OSRAM® SFH 4283 IR 880 nm.

2.3 Detector

Photodetectors are basically modelled as rectangular detector surfaces. In our simulations, the field of view (FOV) and area of photodetectors are assumed to be 90° and 1 cm^2, respectively.

2.4 Channel Impulse Response (CIR)

After we create the simulation environment in Zemax®, we use its non-sequential ray tracing feature to model the channel. In ray tracing approach, rays are traced along a physically realizable path until they intercept an object. The line-of-sight (LOS) response is straightforward to obtain and depends upon the LOS distance. Besides the LOS component, there is a large number of reflections among ceiling, walls, and floor as well as any other objects within the environment. Zemax® non-sequential ray tracing tool generates an output file, which includes the detected power and path lengths from source to detector for each ray. Using this information, we can express the CIR as

$$h(t) = \sum_{i=1}^{N_r} P_i \delta(t - \tau_i) \tag{1}$$

where P_i is the power of the i^{th} ray, τ_i is the propagation time of the i^{th} ray, $\delta(t)$ is the Dirac delta function and N_r is the number of rays received at the detector.

3. NUMERICAL RESULTS AND DISCUSSION

In this study, we carried out our simulation study for 15 configurations (see Section 2) under consideration. The resulting CIRs are provided in Figure 4. It should be noted that we provide CIRs for both IR and VL sources. For easy identification, they are labeled as VLx and IRx where x=1, 2,…, 15 denotes each of the configurations illustrated in Fig.1.

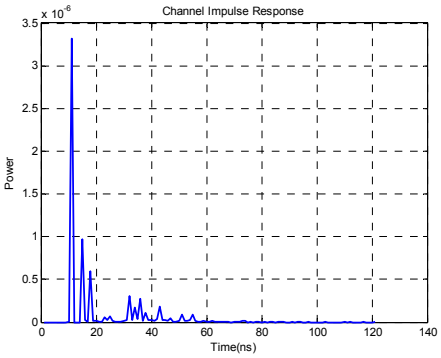

(VL1)

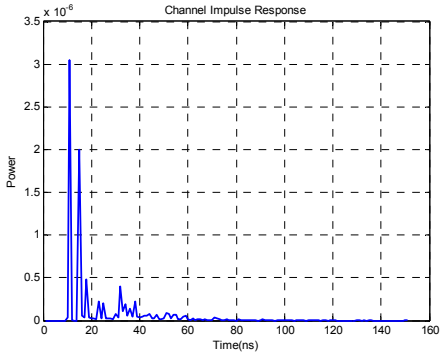

(IR1)

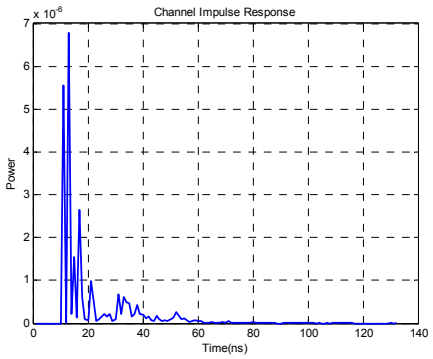

(VL2)

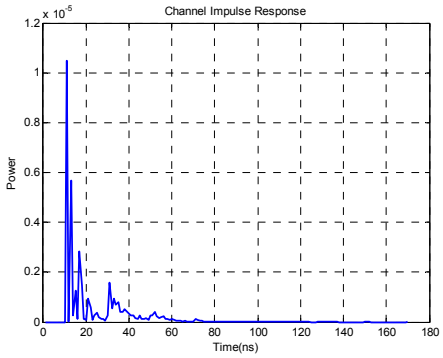

(IR2)

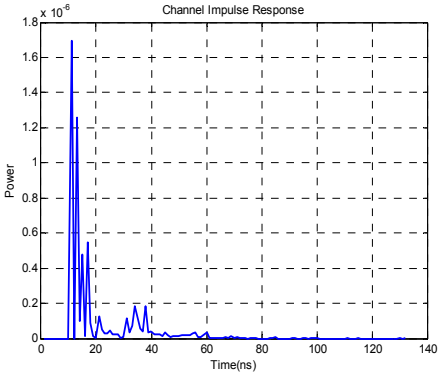

(VL3)

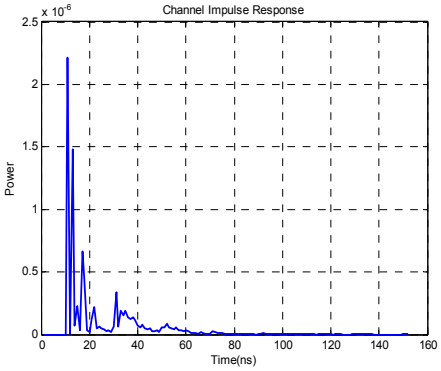

(IR3)

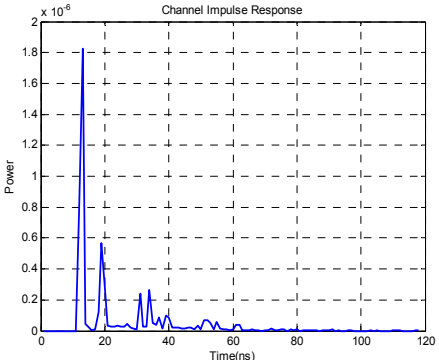

(VL4)

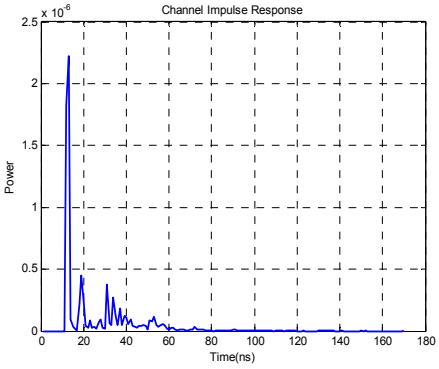

(IR4)

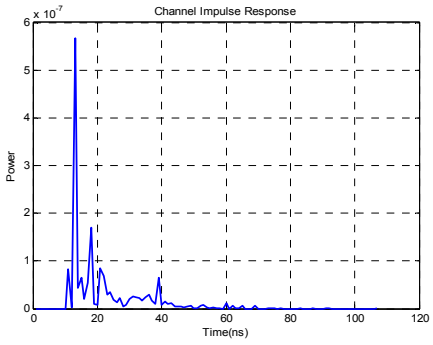

(VL5)

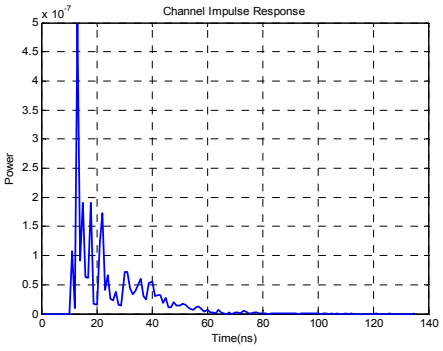

(IR5)

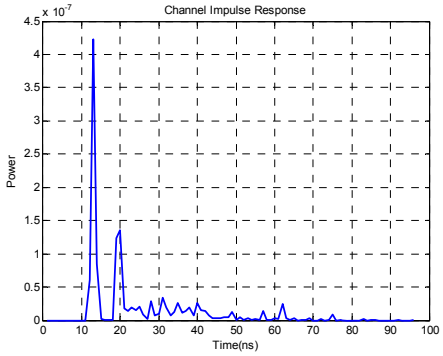

(VL6)

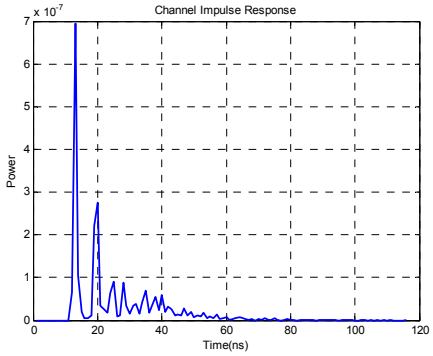

(IR6)

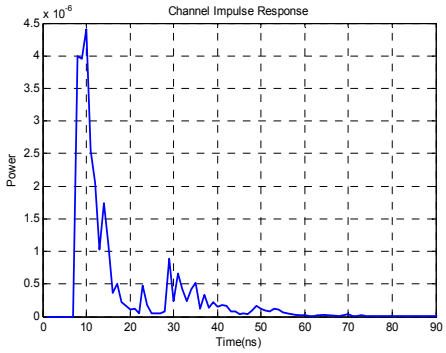

(VL7)

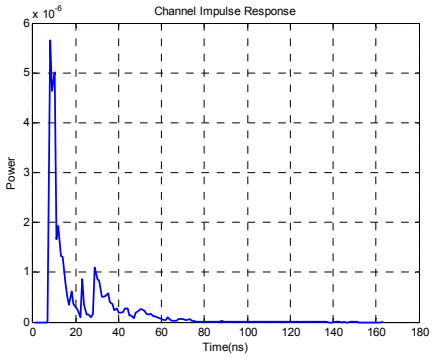

(IR7)

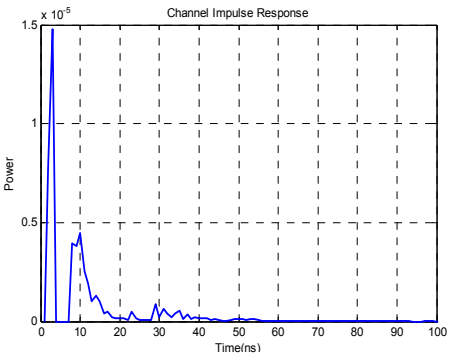

(VL8)

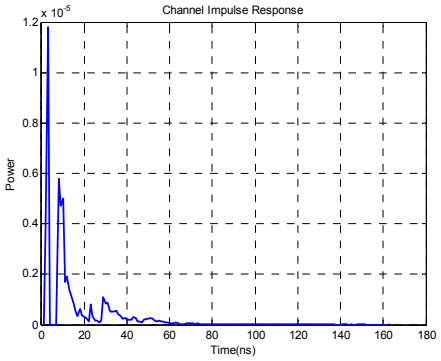

(IR8)

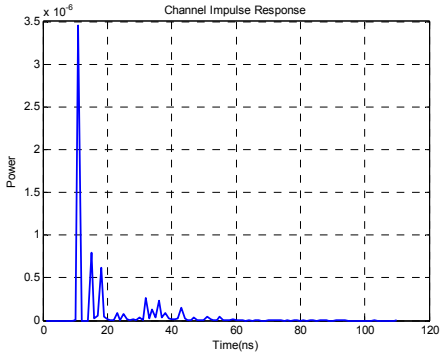

(VL9)

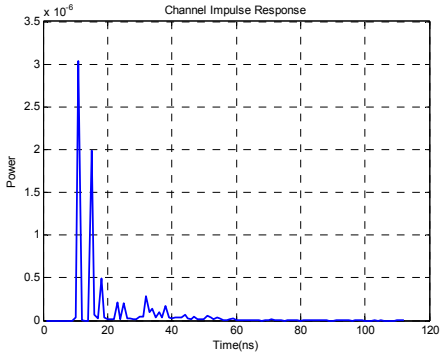

(IR9)

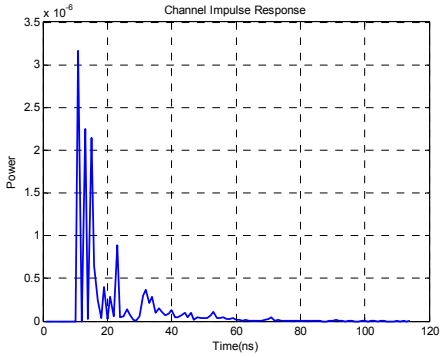

(VL10)

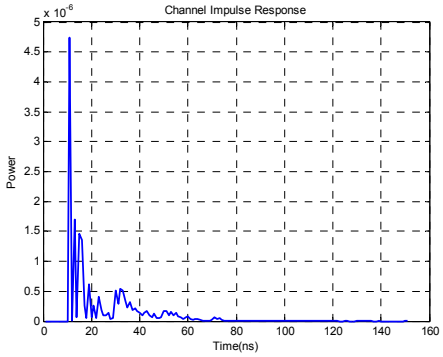

(IR10)

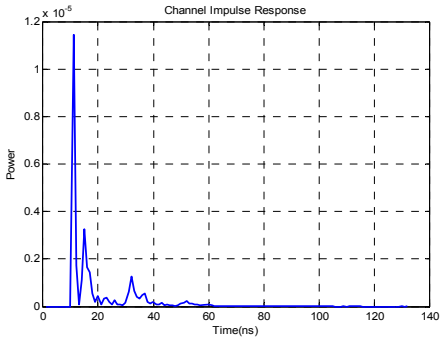

(VL11)

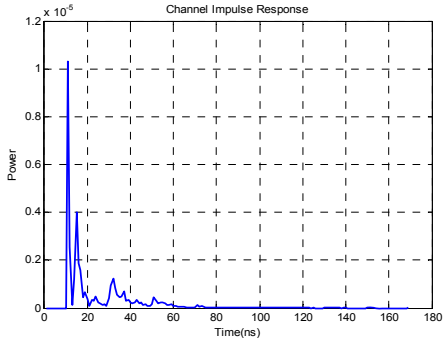

(IR11)

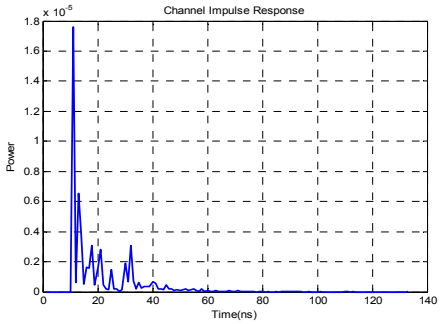

(VL12)

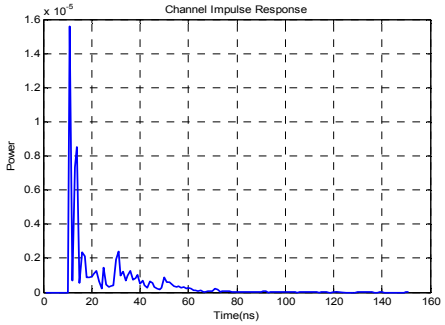

(IR12)

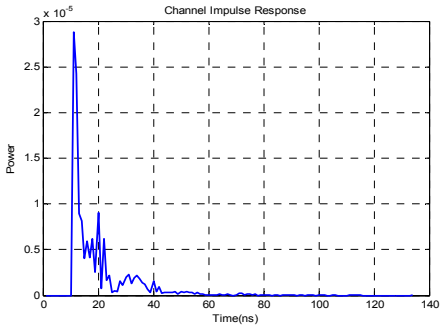

(VL13)

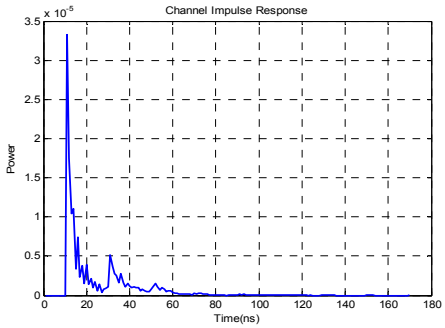

(IR13)

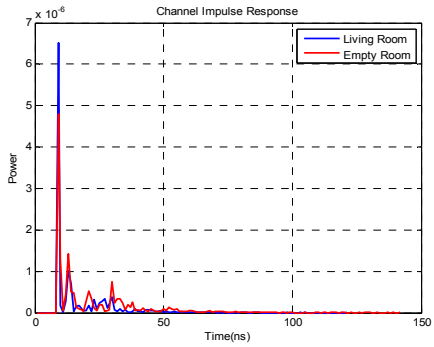

(VL14, 15)

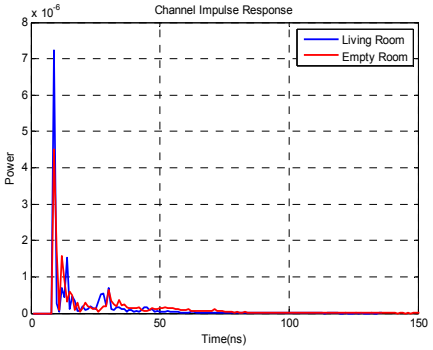

(IR14, 15)

Figure 4. VL and IR channel impulse responses for 15 configurations under consideration.

Based on the obtained CIRs, we further quantify fundamental channel characteristics. Channel DC gain (H_0) is one of the most important features of a VLC channel, as it determines the achievable signal-to-noise ratio for fixed transmitter power. The temporal dispersion can be expressed by the mean excess delay (τ_0) and the channel root mean square (RMS) delay spread (τ_{RMS}) [13], [20]. These channel parameters are calculated based on CIRs and presented in Table 1. Some main observations are further summarized below:

Effect of multi-transmitter deployment: The RMS delay spread of the configuration with single transmitter (VL1) is 13.98 ns while this value in the configuration with four transmitters (VL2) is 14.4 ns indicating an increase of 0.42 ns. This is as a result of additional multipath propagation in the case of multiple transmitters. It is also observed that by increasing the number of illuminators from two to sixteen (VL10-VL13), DC gain increases from 1.35×10^{-5} to 1.40×10^{-4}.

Effect of position/rotation of transmitter/receiver: The position of receiver and transmitter with respect to each other has large effect on channel parameters. For example, in the configuration with receiver at the center (VL1), the RMS delay spread is 13.98 ns and this increases to 15.19 ns in the configuration with detector at the corner (VL4). By moving the detector to the corner, RMS delay increases because the detector receives more scattering from corner sides. The rotation also results in some slight increase and the value of RMS delay spread is calculated as 14.07 ns in configuration VL6. It is also observed that in the configurations with the no-rotation detector (VL3 and VL4) DC gains are 5.89×10^{-6} and 5.54×10^{-6}, and these decrease to 1.69×10^{-6} and 1.30×10^{-6} in the configurations with the rotated detector (VL5 and VL6) because the detector receive less scattering.

Effect of desk light: In the configuration without desk light (VL7), the RMS delay spread is 12.92 ns while this value in the configuration with desk light (VL8) is 12.17 ns indicating a decrease of 0.75 ns. In VL8, the desk light is more close to the detector than the other four transmitters mounted on the ceiling so the dominant transmitter becomes desk light. It can be interpreted that in VL8 we have single effective transmitter while in VL7 we have four transmitters so the RMS delay spread in VL8 is smaller.

Effect of surface materials: In configuration VL9, we use the floor specification from [17] which has smaller reflectivity compared to pine wood floor used in configuration VL1. It is observed that the RMS delay decreases from 13.98 ns to 11.86 ns because the detector receives less power from scattering components.

Effect of furniture: In the configuration with furniture (VL15), we observe that the furniture in the room has decreased delay spread and DC gain. However, it should be noted that depending on relative positions of source, detector and furniture, different observations on CIR can made as noted in an earlier IR channel modelling study [21].

IR vs. VL Channel Models: Comparison of CIRs obtained for IR and VL (see Figure 4) reveals that RMS delay and DC gain of IR channels is larger than those in VL channels for the same configurations. This is due to the reason that reflectivity values in IR band are larger than those in VL band (see Figure 2).

4. CONCLUSIONS

In this paper, we have carried out a VL and IR channel characterization study using non-sequential ray tracing approach. We have obtained CIRs for various indoor environments assuming empty/furnished rectangular rooms with different number of illuminators, wall/object materials and various transmitter/receiver location and rotation. Our results have demonstrated that multi-transmitter deployment results in an increase of delay spread. It is also observed that the position of receiver and transmitter with respect to each other has large effect on channel parameters. For example, by moving the detector to the corner, delay spread increases because the detector receives more scattering from corner sides. Similar effect is also observed when the detector rotation changes. Our results have further pointed out the effect of surface materials. When a floor type with smaller reflectivity is used, due to less scattering, the delay spread has significantly decreased. One-to-one comparisons between IR and VL channels for the same configurations further reveals out that the RMS delay of IR channels is larger than that of VL channels.

Table 1. Channel parameters of different configurations in VL and IR band.

Channel Parameters / Config.	T_{tr} (ns)	t_0 (ns)	t_{RMS} (ns)	H_0
VL1	54	20.48	13.98	6.93×10^{-6}
VL2	54	21.03	14.4	2.62×10^{-5}
IR1	61	22.94	16.19	8.85×10^{-6}
IR2	60	23.53	16.70	3.70×10^{-5}
VL3	55	20.34	13.61	5.89×10^{-6}
VL4	60	23.33	15.19	5.54×10^{-6}
VL5	52	21.70	11.94	1.69×10^{-6}
VL6	61	23.51	14.07	1.30×10^{-6}
IR3	60	23.64	16.05	8.50×10^{-6}
IR4	62	24.41	16.64	8.18×10^{-6}
IR5	56	25.24	13.75	2.65×10^{-6}
IR6	58	25.12	14.12	2.51×10^{-6}
VL7	50	17.34	12.92	2.94×10^{-5}
VL8	42	10.94	12.17	5.12×10^{-5}
IR7	58	20.47	15.98	3.73×10^{-5}
IR8	54	15.17	15.62	5.30×10^{-5}
VL9	47	18.70	11.86	6.62×10^{-6}
IR9	51	19.61	12.38	7.87×10^{-6}
VL10	54	20.94	13.19	1.35×10^{-5}
VL11	53	20.04	13.08	3.07×10^{-5}
VL12	50	20.13	12.21	5.58×10^{-5}
VL13	49	19.41	11.64	1.40×10^{-4}
IR10	61	24.25	16.20	1.76×10^{-5}
IR11	60	23.35	16.05	3.65×10^{-5}
IR12	61	24.28	16.33	6.88×10^{-5}
IR13	59	23.05	15.82	1.50×10^{-4}
VL14	60	21.03	15.81	1.55×10^{-5}
VL15	45	16.04	11.03	1.25×10^{-5}
IR14	74	25.43	20.67	1.87×10^{-5}
IR15	53	18.91	13.85	1.69×10^{-5}

APPENDIX

Config.	Specifications	Room size (m^3)	Position of Transmitters (m)	Position of Receiver (m)	Reflectivity (VL)	Reflectivity (IR)
VL1 IR1 (1)	Empty Room 1 Illuminator	3×3×3	(0,0,3)	(0,0,0)	Wall: Plaster Ceiling: Plaster Floor: Pine Wood	Wall: 83% Ceiling: 83% Floor: 91%
VL2 IR2 (2)	Empty Room 4 Illuminators	3×3×3	(0.75,0.75,3) (0.75,-0.75,3) (-0.75,0.75,3) (-0.75,-0.75,3)	(0,0,0)	Wall: Plaster Ceiling: Plaster Floor: Pine Wood	Wall: 83% Ceiling: 83% Floor: 91%
VL3 IR3 (3)	Empty Room 1 Illuminator (Corner)	3×3×3	(0,0,3)	(0.75,0.75,0)	Wall: Plaster Ceiling: Plaster Floor: Pine Wood	Wall: 83% Ceiling: 83% Floor: 91%
VL4 IR4 (4)	Empty Room 1 Illuminator (Corner)	3×3×3	(0,0,3)	(1.3,1.3,0)	Wall: Plaster Ceiling: Plaster Floor: Pine Wood	Wall: 83% Ceiling: 83% Floor: 91%
VL5 IR5 (5)	Empty Room 1 Illuminator (Rotation)	3×3×3	(0,0,3)	(0.75,0.75,0)	Wall: Plaster Ceiling: Plaster Floor: Pine Wood	Wall: 83% Ceiling: 83% Floor: 91%
VL6 IR6 (6)	Empty Room 1 Illuminator (Rotation)	3×3×3	(0,0,3)	(1.3,1.3,0)	Wall: Plaster Ceiling: Plaster Floor: Pine Wood	Wall: 83% Ceiling: 83% Floor: 91%
VL7 IR7 (7)	Room without Desk Light 4 Illuminators	3×3×3	(0.75,0.75,3) (0.75,-0.75,3) (-0.75,0.75,3) (-0.75,-0.75,3)	(-1.02,1.14,0.76)	Wall: Plaster Ceiling: Plaster Floor: Pine Wood Desk: Pine Wood	Wall: 83% Ceiling: 83% Floor: 91% Desk: 91%
VL8 IR8 (8)	Room with Desk Light 4 Illuminators	3×3×3	(0.75,0.75,3) (0.75,-0.75,3) (-0.75,0.75,3) (-0.75,-0.75,3) (-0.55,1.09,1.04)	(-1.02,1.14,0.76)	Wall: Plaster Ceiling: Plaster Floor: Pine Wood Desk: Pine Wood Desk Lamp: Black Gloss Paint	Wall: 83% Ceiling: 83% Floor: 91% Desk: 91% Desk Lamp: 3.7%
VL9 IR9 (9)	Different Material Types	3×3×3	(0,0,3)	(0,0,0)	Wall: Plaster Ceiling: Plaster Floor: from [17]	Wall: 83% Ceiling: 83% Floor: 63%
VL10 IR10 (10)	Empty Room MIMO-VLC	3×3×3	(0.75,0,3) (-0.75,0,3)	(0,0,0)	Wall: Plaster Ceiling: Plaster Floor: Pine Wood	Wall: 83% Ceiling: 83% Floor: 91%
VL11 IR11 (11)		3×3×3	(0.375,0,3) (-0.375,0,3) (1.125,0,3) (-1.125,0,3)	(0,0,0)	Wall: Plaster Ceiling: Plaster Floor: Pine Wood	Wall: 83% Ceiling: 83% Floor: 91%
VL12 IR12 (12)		3×3×3	(0.375,0.75,3) (1.125,0.75,3) (0.375,-0.75,3) (1.125,-0.75,3) (-0.375,0.75,3) (-1.125,0.75,3) (-0.375,-0.75,3) (-1.125,-0.75,3)	(0,0,0)	Wall: Plaster Ceiling: Plaster Floor: Pine Wood	Wall: 83% Ceiling: 83% Floor: 91%
VL13 IR13 (13)		3×3×3	(0.375,0.375,3) (1.125,0.375,3) (0.375,-0.375,3) (1.125,-0.375,3) (-0.375,0.375,3) (-1.125,0.375,3) (-0.375,-0.375,3) (-1.125,-0.375,3) (0.375,1.125,3) (1.125,1.125,3) (0.375,-1.125,3) (1.125,-1.125,3) (-0.375,1.125,3) (-1.125,1.125,3) (-0.375,-1.125,3) (-1.125,-1.125,3)	(0,0,0)	Wall: Plaster Ceiling: Plaster Floor: Pine Wood	Wall: 83% Ceiling: 83% Floor: 91%
VL14 IR14 (14)	Empty Room	4.2×5.5×3	(1.05,1.375,2.9) (1.05,-1.375,2.9) (-1.05,1.375,2.9) (-1.05,-1.375,2.9)	(1.6,1.6,0.75)	Wall: Plaster Ceiling: Plaster Floor: Pine Wood	Wall: 83% Ceiling: 83% Floor: 91%
VL15 IR15 (15)	Living Room				Wall/Ceiling: Plaster Floor: Pine Wood Furniture: Pine Wood Window: Glass TV: Black Gloss Paint Radiator: Aluminum	Wall/Ceiling: 83% Floor: 91% Furniture: 91% Window: 8.5% TV: 3.7% Radiator: 53%

REFERENCES

[1] Arnon, S., Barry, J. R., Karagiannidis, G. K., Schober, R. and Uysal, M. (Eds.), [Advanced Optical Wireless Communication], 1st ed., Cambridge University Press, pp. 353-368, (2012).

[2] Komine, T. and Nakagawa, M., "Fundamental analysis for visible light communications using LED lights," IEEE Trans. on Consumer Electronics, vol. 50, no. 1, pp. 100-107, Feb. (2004).

[3] Hong, Y., Chen, J., Wang, Z. and Yu, C., "Performance of a precoding MIMO system for decentralized multiuser indoor visible light communications," IEEE Photon. J., vol. 5, no. 4, (2013).

[4] Jovicic, A., Li, J. and Richardson, T., "Visible light communication: opportunities, challenges and the path to market," IEEE Commun. Mag., vol. 51, no. 12, pp. 26–32, (2013).

[5] Gancarz, J., Elgala, H. and Little, T. D. C., "Impact of lighting requirements on VLC systems," IEEE Commun. Mag., vol. 51, no. 12, pp. 34–41, (2013).

[6] Bykhovsky, D. and Arnon, S., "Multiple access resource allocation in visible light communication systems," J. Lightw. Technol., vol. 32, no. 8, pp. 1594–1600, (2014).

[7] Gfeller, F. R. and Bapst, U. H., "Wireless In-House Data Communication via Diffuse Infrared Radiation," Proc. IEEE, vol. 67, no. 11, pp. 1474–1486, Nov. (1979).

[8] Barry, J. R., [Wireless Infrared Communications], Kluwer Academic, (1994).

[9] Kahn, J. M., Krause, W. J. and Carruthers, J. B., "Experimental Characterization of Non-directed Indoor Infrared Channels," IEEE Trans. Commun., vol. 43, no. 234, pp. 1613–1623, Apr. (1995).

[10] Chun, H., Chiang, C. and O'Brien, D., "Visible Light Communication Using OLEDs: Illumination and Channel Modeling," in Int. Workshop Opt. Wireless Commun., pp. 1–3, Oct. (2012).

[11] Nguyen, H. Q. et al., "A MATLAB-Based Simulation Program for Indoor Visible Light Communication System," CSNDSP 2010, pp. 537-540, July (2010).

[12] Komine, T. and Nakagawa, M., "Performance Evaluation on Visible-light Wireless Communication System Using White LED Lightings," in Proc. Ninth IEEE Symposium on Computers and Communications, vol. 1, pp. 258-263, (2004).

[13] Sarbazi, E. and Uysal, M., Abdallah, M. and Qaraqe, K., "Indoor Channel Modeling and Characterization for Visible Light Communications," Invited Paper, 16th International Conference on Transparent Optical Networks (ICTON), Graz, Austria, July 2014.

[14] "Zemax 13 Release 2, Radiant Zemax LLC," www.radiantzemax.com/zemax.

[15] "GrabCAD models," [Online]. Available at: https://grabcad.com.

[16] "ASTER Spectral Library - Version 2.0," [Online]. Available at: http://speclib.jpl.nasa.gov.

[17] Lee, K., Park, H. and Barry, J. R., "Indoor Channel Characteristics for Visible Light Communications," IEEE Commun. Lett., vol. 15, no. 2, Feb (2011).

[18] "CREE LEDs," [Online]. Available at: http://www.cree.com.

[19] "OSRAM LEDs," [Online]. Available at: http://www.osram-os.com.

[20] Sarbazi, E., Uysal, M., Abdallah, M. and Qaraqe, K., "Ray Tracing Based Channel Modeling for Visible Light Communications," IEEE 22nd Signal Processing, Communication and Applications Conference (SIU), Trabzon, Turkey, April 2014.

[21] Abtahi, M. and Hashemi, H., "Simulation of indoor propagation channel at infrared frequencies in furnished office environments," in PIMRC, pp. 306–310, (1995).